On the Reduction of Basic Iron Acetate: Isolation of Ferrous Species Mediating Gif-Type Oxidation of Hydrocarbons

4 AUTHORS, INCLUDING:

Georgia Papaefthymiou
Villanova University
153 PUBLICATIONS **6,789** CITATIONS

SEE PROFILE

On the Reduction of Basic Iron Acetate: Isolation of Ferrous Species Mediating Gif-Type Oxidation of Hydrocarbons

Bharat Singh,[1a] Jeffrey R. Long,[1b]
Georgia C. Papaefthymiou,[1c] and Pericles Stavropoulos*,[1a]

Department of Chemistry, Boston University
Boston, Massachusetts 02215
Department of Chemistry, Harvard University
Cambridge, Massachusetts 02138
Francis Bitter Magnet Laboratory
Massachusetts Institute of Technology
Cambridge, Massachusetts 02139

Scheme 1

Structurally unspecified iron species have been implicated in the hydrocarbon-oxidizing Fenton,[2] Udenfriend,[3] and Gif[4] systems. Early versions[5] of the Gif system were based on dioxygen activation by ferrous species in pyridine/acetic acid (py/AcOH) solutions. The choice of solvents and the selectivity for the ketonization/hydroxylation of certain substrates[6] suggest that structural/functional similarities, but also discrepancies,[6c] may exist between active Gif reagents and the diiron site of the hydroxylase component of soluble methane monooxygenase (sMMO).[7] To investigate these assumptions, we have selected the basic iron acetate $[Fe_3O(O_2CCH_3)_6(py)_3] \cdot py$ (**1**) (Gif^{IV})[8] as a point of departure. Pertinent transformations explored in this study are summarized in Scheme 1.

Reduction (30 min) of 0.40 mmol of brown-black **1**[9] with excess Zn in 5.0 mL of $CH_3CN/AcOH$ (10:1 or 2:1 v/v) or $CH_2Cl_2/AcOH$ (10:1) results in the precipitation (−20 °C) of light yellow crystals of $[Zn_2Fe^{II}(O_2CCH_3)_6(py)_2]$ (**2**, 65%).[10] The analogous reduction of **1** in py/AcOH (10:1 or 5:1) affords yellow-green crystals of $[Fe^{II}(O_2CCH_3)_2(py)_4]$ (**3**, 80%).[10,11] In contrast, diffusion of Et_2O into the original py/AcOH filtrates at 10 °C yields yellow crystals of $[Fe^{II}_2(O_2CCH_3)_4(py)_3]_n$ (**4**,
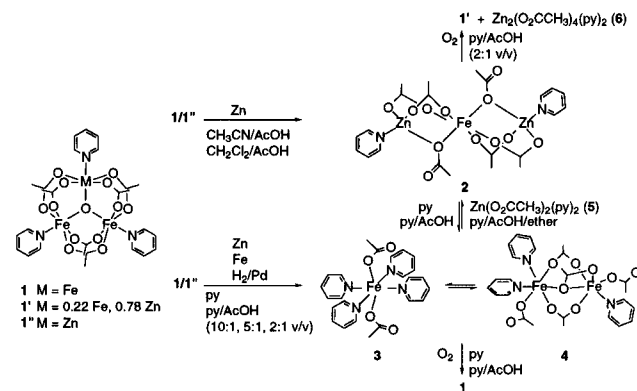
40%).[10] These are occasionally contaminated with **3** (py/AcOH 10:1), **2** (py/AcOH 5:1), and colorless crystals of $[Zn(O_2CCH_3)_2-(py)_2]$ (**5**).[12] Addition of a large excess of Et_2O to the py/AcOH reaction filtrates favors the formation of **2**. Clearly, enrichment in AcOH and/or Et_2O shifts the pyridine-dependent equilibria in the order **3** → **4** → **2**. Pure **2** is obtained by diffusion of Et_2O into the filtrate of the reduction of **1** with Zn in py/AcOH (2:1). Feathery crystals of **4** are obtained pure from concentrated solutions of **3** in py/AcOH (5:1, 2:1) upon addition of Et_2O. Crystals of **4** suitable for X-ray analysis could only be prepared from **3** in py/Et_2O(excess) at 10 °C. In neat pyridine, the reduction (6 h) of **1** with Zn yields **3** (80%, −20 °C) and a small amount of a brown-black film. Attempts to crystallize the latter material, which retains Fe(III) according to ^{57}Fe Mössbauer data, have been unsuccessful. Species **3** and **4** are also obtained by treatment of **1** with iron dust or with H_2 (30 psig)/Pd in py or py/AcOH (10:1). A control experiment confirmed that compounds **3** and **4** are also generated by stirring Fe in py/AcOH.

Upon exposure of their py or py/AcOH solutions to pure dioxygen or air, both **3** and **4** are quantitatively converted to **1**. The reaction of **2** with dioxygen in py/AcOH (2:1) yields red-black crystals of $[Fe_{2.22(2)}Zn_{0.78(2)}O(O_2CCH_3)_6(py)_3] \cdot py$ (**1′**)[10] (95%) and colorless crystals of $[Zn_2(O_2CCH_3)_4(py)_2]$ (**6**, 75%).[12] Compound **1′** is distinguished from **1** by its ^1H NMR, ^{57}Fe Mössbauer data (10% Fe(II)), and Fe/Zn ICP microanalyses.[10] Electron microprobe analysis confirmed that each individual crystal of **1′** contains zinc (Fe:Zn = 74:26).[13] Admitting dioxygen to the filtrate of the reduction (6 h) of **1** by Zn in py generates $[Fe_2ZnO(O_2CCH_3)_6(py)_3] \cdot py$ (**1″**).[14] Analogous treatment of **1″** with Zn dust yields results nearly identical to those described for **1**.

Species **2**, **3**, **4**, and **5** are related by equilibria. When dissolved in py or py/AcOH, **2** affords quantitative amounts of **3** and **5** at −20 °C. Conversely, 0.5 mmol of **3** and 1.0 mmol of **5** in py or py/AcOH deposit pure **2** *upon addition of Et_2O*. Absorption spectra of **2** in py or py/AcOH indicate a greater than 90% conversion to **3/4**. The UV−vis spectrum of **3** in py (λ_{max} 396 nm (ϵ_M = 2107); Beer's law observed ([**3**] < 1.0 × 10^{-3} M)) exhibits a new broad absorption (λ_{max} 424 nm) at higher concentrations. In the near-IR region, concentrated solutions of **3** (10^{-1} M) or filtrates of the reduction of **1** by Zn dust in py or py/AcOH demonstrate broad d−d transition bands

(1) (a) Boston University. (b) Harvard University. (c) Massachusetts Institute of Technology.

(2) (a) Walling, C. *Acc. Chem. Res.* **1975**, *8*, 125−131. (b) Stubbe, J.; Kozarich, J. W. *Chem. Rev.* **1987**, *87*, 1107−1136. (c) Sawyer, D. T.; Kang, C.; Llobet, A.; Redman, C. *J. Am. Chem. Soc.* **1993**, *115*, 5817−5818.

(3) Udenfriend, S.; Clark, C. T.; Axelrod, J.; Brodie, B. B. *J. Biol. Chem.* **1954**, *208*, 731−739.

(4) Barton, D. H. R.; Doller, D. *Acc. Chem. Res.* **1992**, *25*, 504−512.

(5) Barton, D. H. R.; Bévière, S. D.; Chavasiri, W.; Csuhai, E.; Doller, D.; Liu, W.-G. *J. Am. Chem. Soc.* **1992**, *114*, 2147−2156.

(6) (a) Barton, D. H. R.; Boivin, J.; Motherwell, W. B.; Ozbalik, N.; Schwartzentruber, K. M.; Jankowski, K. *New J. Chem.* **1986**, *10*, 387−398. (b) Green, J.; Dalton, H. *J. Biol. Chem.* **1989**, *264*, 17698−17703. (c) Froland, W. A.; Andersson, K. K.; Lee, S.-K.; Liu, Y.; Lipscomb, J. D. *J. Biol. Chem.* **1992**, *267*, 17588−17597.

(7) (a) Liu, K. E.; Valentine, A. M.; Wang, D.; Huynh, B. H.; Edmondson, D. E.; Salifoglou, A.; Lippard, S. J. *J. Am. Chem. Soc.* **1995**, *117*, 10174−10185. (b) Lipscomb, J. D. *Annu. Rev. Microbiol.* **1994**, *48*, 371−399.

(8) Barton, D. H. R.; Boivin, J.; Gastiger, M.; Morzycki, J.; Hay-Motherwell, R. S.; Motherwell, W. B.; Ozbalik, N.; Schwartzentruber, K. M. *J. Chem. Soc., Perkin Trans. 1* **1986**, 947−955.

(9) Sorai, M.; Kaji, K.; Hendrickson, D. N.; Oh, S. M. *J. Am. Chem. Soc.* **1986**, *108*, 702−708.

(10) Analytical, spectroscopic and detailed crystallographic data have been deposited as supporting information. Crystal data for **1′**, *R32*, a = 17.556(4) Å, c = 10.932(5) Å, V = 2918(2) Å³, T = 223 K, Z = 3, R = 0.0416, R_w = 0.0461; **2**, $P2_1/n$, a = 10.255(2) Å, b = 10.756(2) Å, c = 12.727(3) Å, β = 95.56(3)°, V = 1397.2(5) Å³, T = 223 K, Z = 2, R = 0.0334, R_w = 0.0362; **3**, *Pccn*, a = 8.857(7) Å, b = 16.401(9) Å, c = 16.653(10) Å, V = 2419(3) Å³, T = 223 K, Z = 4, R = 0.0391, R_w = 0.0383; **4**, $Pna2_1$, a = 16.018(4) Å, b = 9.687(3) Å, c = 18.107(6) Å, V = 2810(1) Å³, T = 295 K, Z = 4, R = 0.0388, $wR2$ = 0.0887.

(11) **3** has been previously synthesized from Fe(II) precursors, but details of its synthesis and/or characterization were unclear: (a) Catterick, J.; Thornton, P.; Fitzsimmons, B. W. *J. Chem. Soc., Dalton Trans.* **1977**, 1420−1425. (b) Hardt, H.-D.; Möller, W. *Z. Anorg. Allg. Chem.* **1961**, *313*, 57−69. (c) Sheu, C.; Richert, S. A.; Cofré, Ross, B., Jr.; Sobkowiak, A.; Sawyer, D. T.; Kanofsky, J. R. *J. Am. Chem. Soc.* **1990**, *112*, 1936−1942.
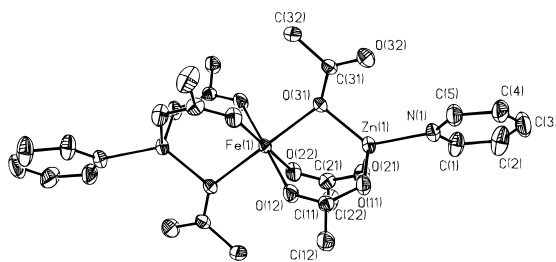
(12) $Zn(O_2CCH_3)_2 \cdot 2H_2O$ consistently crystallizes as $[Zn(O_2CCH_3)_2(py)_2]$ (**5**) from py or py/AcOH (10:1, 5:1) and as $[Zn_2(O_2CCH_3)_4(py)_2]$ (**6**) from py/AcOH (2:1). Structural details will be published elsewhere.

(13) This result along with preliminary powder X-ray diffraction analysis of **1**, **1′** and **1″** render it unlikely that domains of **1** and **1″** are present in the structure of **1′**. Also see: Jang, H. G.; Kaji, K.; Sorai, M.; Wittebort, R. J.; Geib, S. J.; Rheingold, A. L.; Hendrickson, D. N. *Inorg. Chem.* **1990**, *29*, 3547−3556.

(14) Blake, A. B.; Yavari, A.; Hatfield, W. E.; Sethulekshmi, C. N. *J. Chem. Soc., Dalton Trans.* **1985**, 2509−2520.

Figure 1. ORTEP diagram of **2** showing 40% probability ellipsoids and atom-labeling schemes.
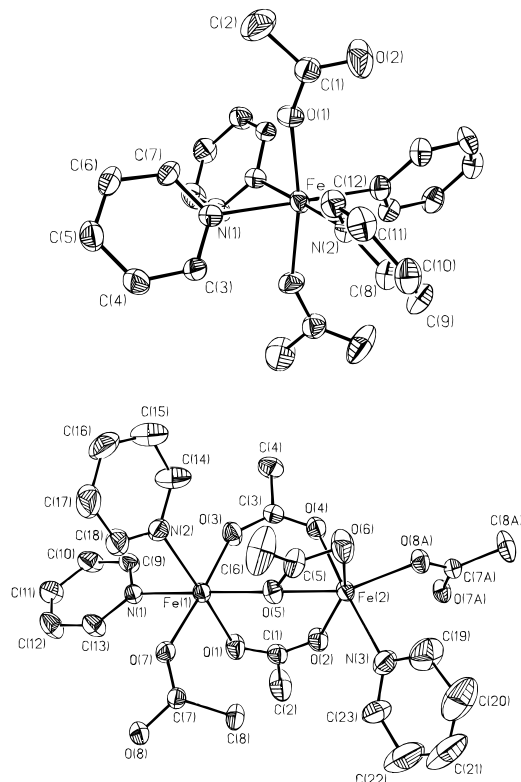

Figure 2. ORTEP diagrams of **3** (top) and **4** (bottom) showing 50% and 30% probability ellipsoids, respectively, and atom-labeling schemes.

($\lambda_{max} \approx 850$ ($\epsilon_M \approx 8$), 1180 ($\epsilon_M \approx 8$) nm) which are almost identical to those exhibited in near-IR/ATR (ATR = attenuated total internal reflectance) spectra of solid **4**.

Compound **1'** (supporting information) crystallizes in space group $R32$ featuring trinuclear μ-oxo units with crystallographically imposed D_3 symmetry (at 223 K cluster disorder does not allow the different metal sites to be distinguished). The structure of **2** (Figure 1) features a linear arrangement of the metal centers, with the centrosymmetric iron atom bridged, via two bidentate and one monodentate acetate groups, to the tetrahedrally ligated zinc atoms. The structure of **3** (Figure 2) reveals a distorted octahedral Fe environment with an imposed C_2 axis bisecting the equatorial plane defined by the four Fe−N bonds. Pyridine rings are arranged in a propeller fashion, while acetates assume

trans positions along the propeller axis (O(1)−Fe−O(1') = 168.5(2)°). The structure of **4** (Figure 2) reveals a one-dimensional chain comprised of asymmetric diferrous units. The octahedral Fe(1) atom is bridged by three acetate groups to a more distorted Fe(2) site (Fe(1)···Fe(2) = 3.676 Å). The distortion arises due to the bidentate chelation of the unique monodentate acetate bridge[15] to Fe(2) (Fe(2)−O(6) = 2.273(5) Å). Each dinuclear unit is bridged to two adjacent units via O(8) and O(7A) (Fe(1)···Fe(2') = 5.275 Å).

The zero-field ^{57}Fe Mössbauer spectrum of **4** in the solid state at 4.2 K does not distinguish between the two iron sites (δ = 1.27 mm/s, ΔE_Q = 2.92 mm/s, Γ = 0.20 mm/s).[16] The temperature dependence of the magnetic moment of **4** (μ_{eff}^{corr} = 7.07 μ_B (300 K), 2.58 μ_B (2 K)) is suggestive of antiferro-magnetically coupled ferrous sites within the dinuclear unit.[17]

Catalytic oxidation of adamantane mediated by **2**−**4** under Gif conditions (adamantane (100 mg)/catalyst (10 mg)/Zn (1.3 g)/air) in py (27 mL)/AcOH (2.7 mL) for 18 h yields similar results to those previously reported[6a] for **1**. The adamantane-based products, analyzed by GC and GC−MS, include 2-ada-mantanone (**2**, 11.7%; **3**, 11.3%; **4**, 10.1%), 2-adamantanol (**2**, 1.4%; **3**, 1.3%; **4**, 1.3%), 1-adamantanol (**2**, 0.5%; **3**, 0.6%; **4**, 0.7%), 4-(1-adamantyl)pyridine (**2**, 5.4%; **3**, 5.8%; **4**, 6.0%), and 2-(1-adamantyl)pyridine (**2**, 3.2%; **3**, 3.3%; **4**, 3.2%). The preference for secondary over tertiary carbons (C_2/C_3) is in the range 1.2−1.4.

This study provides an inorganic template to place Gif chemistry on a rational basis. Structure **4** relates favorably to the asymmetric diferrous site of sMMO.[18] However, any genuine relation to the active site of sMMO needs to be drawn on the basis of the geometric features of the active oxidant involved. This point, along with the question of whether the present ferrous compounds are kinetically competent to mediate oxidation of hydrocarbons, will be the subject of future investigations.

Supporting Information Available: Text describing analytical and spectroscopic data and tables containing listings of crystal and data collection parameters, atomic coordinates and isotropic thermal parameters, interatomic distances, bond angles, and anisotropic displacement parameters for **1'**, **2**, **3**, and **4** (27 pages). Ordering information is given on any current masthead page.

JA960529P

(15) (a) Goldberg, D. P.; Telser, J.; Bastos, C. M.; Lippard, S. J. *Inorg. Chem.* **1995**, *34*, 3011−3024. (b) Rardin, R. L.; Tolman, W. B.; Lippard, S. J. *New J. Chem.* **1991**, *15*, 417−430.

(16) For a similar result on a closely related compound, see: Coucouvanis, D.; Reynolds, R. A., III; Dunham, W. R. *J. Am. Chem. Soc.* **1995**, *117*, 7570−7571.

(17) Evaluation of the exchange coupling constant(s) *J* for the one-dimensional solid **4** is in progress.

(18) Rosenzweig, A. C.; Nordlund, P.; Takahara, P. M.; Frederick, C. A.; Lippard, S. J. *Chem. Biol.* **1995**, *2*, 409−418.